

Synthesis and luminescent properties of block copolymers based on polyfluorene and polytriphenylamine

Ying Tan, Zhijie Gu, Kousuke Tsuchiya, Kenji Ogino*

Graduate School of Bio-Applications and Systems Engineering, Tokyo University of Agriculture and Technology, 2-24-16 Nakacho, Koganei-shi, Tokyo 184-8588, Japan

ARTICLE INFO

Article history:

Received 15 December 2011
Received in revised form
10 February 2012
Accepted 14 February 2012
Available online 21 February 2012

Keywords:

Polyfluorene
Polytriphenylamine
Block copolymer

ABSTRACT

For the preparation of block copolymers containing polyfluorene (PF) and hole transporting segment, PF homopolymers with diphenylamine terminals were synthesized by Suzuki coupling polymerization. The terminals of PF were converted to polytriphenylamine (PTPA) block by C–N coupling polymerization to give PTPA-*block*-PF-*block*-PTPA (PF-PTPA) triblock copolymers with different PTPA chain lengths. These polymers were soluble in common organic solvents and readily formed thin films by solution processing. All of the polymers exhibited similar UV absorption and PL emission properties both in chloroform solution and in film state. PF-PTPA block copolymers showed relatively high HOMO compared with that of PF by cyclic voltammetry. Compared with corresponding PF homopolymers, the EL devices based on PF-PTPA block copolymers showed higher luminance and current efficiency than those of PF homopolymers because of the improvement of hole injection by the introduction of PTPA segment.

© 2012 Elsevier Ltd. All rights reserved.

1. Introduction

Polyfluorenes (PFs), which possess a relatively large band gap, have been widely investigated as a blue PLED material because of their superior properties, such as highly efficient photoluminescence (PL), excellent thermal stability, and good solubility in common organic solvents [1,2]. However, they exhibit insufficient color stability causing troublesome long wavelength emission band (520–560 nm), assigned to aggregates/excimers, interchain interactions, and/or an emissive keto defect generated by thermo-, photo-, or electro-oxidative degradation during device operation [3–6]. In fact, various kinds of modifications were proposed to prepare polyfluorene-based copolymers to improve the performance. For example, an alkyl/phenyl structure was introduced at the C-9 position to reduce the aggregation and keto defect [7–10], or end-capping groups were attached to PF backbones to suppress the green emission by keeping the recombination zone away from the polymer/anode interface and by increasing the hole-trap efficiency [11]. Another serious problem associated with PF is poor electroluminescence (EL) efficiency due to an imbalance in charge carriers caused by large hole injection barriers and different charge carrier mobilities [12]. Therefore, PFs require additional hole-transporting layers to obtain efficient hole injection/transport in EL device.

Triphenylamine (TPA) derivatives have been known as candidates for hole transporting materials to be used in organic EL and photovoltaic cell devices. Many compounds containing the TPA moiety for EL devices have been reported for decades [13–16]. Furthermore, some researchers employed triphenylamine as a polymer backbone for building up the π -conjugated structure of poly(triphenylamine) (PTPA) [17–20] because PTPA has been found to a) facilitate hole injection and transport from the anode and b) serve as an electron-blocking layer, which blocks electron movement to the anode and confines excitons within the emission layer to reduce green emission [5,6]. Previously, we reported that PTPA can be synthesized via C–N coupling polymerization of a self-condensing monomer by palladium catalyst [21]. This technique allows us to assemble PTPA into the block copolymer architectures by the chain elongation from terminals of the other polymer.

Incorporating some functional components such as charge transport and luminescent moieties into a copolymer can easily adjust the balance between hole and electron injections in the emitting layer in polymer EL devices. For example, multilayer blue-emitting EL device based on fluorene-triarylamine alternating copolymer with a high hole mobility showed a high current efficiency as 8.7 cd/A [22]. Moreover, we demonstrated that the device based on bipolar charge transporting block copolymers showed higher external quantum efficiency compared with random copolymers or polymer blends with the same composition [23,24]. The microphase-separated structure built in the block copolymer layer afforded the effective charge recombination [25,26]. The block

* Corresponding author. Tel./fax: +81 42 388 7404.
E-mail address: kogino@cc.tuat.ac.jp (K. Ogino).

copolymer containing polyfluorene segment was also reported by the other authors [27]. In this work, block copolymers consisting of PF and PTPA were synthesized for a luminescent material in EL devices. PTPA segments were introduced at the terminals of PF for improvement of hole injection/transport at the PF layer. In order to convert the terminals of PF to diphenylamine group, polymerization method of the fluorene monomer(s) was optimized. The terminal-modified PFs were sequentially altered to the block copolymers by C–N coupling polymerization. The structures of PF homopolymers and block copolymers were characterized by GPC and ^1H NMR. The photophysical and electrical properties of the polymers as well as performance of the EL device based on them were examined.

2. Experimental

2.1. Materials

All reagents and solvents were used without further purification unless stated otherwise. Tetrahydrofuran (THF) was distilled over sodium and benzophenone, and stored under nitrogen atmosphere. Toluene was distilled over calcium hydride, and stored under nitrogen atmosphere. The other reagents and solvents were obtained commercially and were used as received.

2.2. Synthesis of 2,7-dibromofluorene (**1**)

Fluorene (16.62 g, 0.10 mol), 2,6-*t*-butyl-4-cresol (0.04 g, 0.182 mmol), FeCl_3 (0.4010 g, 2.48 mmol), and chloroform (300 mL) were added into a flask under nitrogen atmosphere and cooled down to -78°C , and then bromine (12.5 mL, 0.244 mmol) was added dropwise slowly. After reaction for 24 h at r.t., NaHSO_3 aq. (300 mL) was added. The product was extracted with chloroform and dichloromethane, and the organic layer was dried with MgSO_4 . After the organic layer was concentrated by rotary evaporator, the crude product was recrystallized from methanol once or twice. White crystal (26.64 g in total) was obtained. The yield was 82%. ^1H NMR (300 MHz, CDCl_3) δ (ppm): 7.68 (s, 2H, ArH), 7.60 (d, $J = 9.0$ Hz, 2H, ArH), 7.52 (d, $J = 9.0$ Hz, 2H, ArH), 3.87 (s, 2H, CH_2). ^{13}C NMR (75 MHz, CDCl_3) δ (ppm): 144.87, 139.78, 130.24, 128.40, 121.30, 121.02, 36.65. HR-MS (m/z): calcd for $\text{C}_{13}\text{H}_8\text{Br}_2$, 321.8993; found, 323.8999 [M] $^+$.

2.3. Synthesis of 2,7-dibromofluorene-9-one (**2**)

To a flask equipped with a stopcock were added **1** (20.0 g, 61.7 mmol) and acetic acid (150 mL) under nitrogen atmosphere. A solution of CrO_3 (15 g, 150 mmol) dissolved in acetic acid (120 mL) was added. After reaction for 24 h at r.t., the solution was neutralized with sodium bicarbonate aq. and the precipitate was filtrated. The crude product was recrystallized from ethanol and chloroform twice. Yellow crystal (10.02 g in total) was obtained. The yield was 48%. ^1H NMR (300 MHz, CDCl_3) δ (ppm): 7.72 (d, $J = 3.0$ Hz, 2H, ArH), 7.60 (dd, $J = 6.0$ Hz, 2H, ArH), 7.35 (d, $J = 9.0$ Hz, 2H, ArH). ^{13}C NMR (75 MHz, CDCl_3) δ (ppm): 191.01, 142.28, 137.57, 135.30, 127.88, 123.42, 121.96. HR-MS (m/z): calcd for $\text{C}_{13}\text{H}_7\text{Br}_2\text{O}$, 336.8864; found, 336.8864 [$\text{M} + \text{H}$] $^+$.

2.4. Synthesis of 2,7-dibromo-9-(4-octylphenyl)fluorene-9-ol (**3**)

To a 100-mL flask equipped with a stopcock and a condenser were placed Mg (0.28 g, 12.0 mmol), 1,2-dibromoethane (0.020 mL, 0.23 mmol), and THF (2.0 mL) under nitrogen atmosphere. When Mg began to react, a solution of 4-bromooctylbenzene (3.0 g, 11 mmol) dissolved in THF (2.0 mL) was added, and the mixture was refluxed until Mg reacted completely. The solution was cooled down to r.t.,

THF (37 mL) and **2** (2.80 g, 8.3 mmol) were added and the mixture was refluxed for 16 h. After reaction for 2 h at r.t., the mixture was treated with saturated NH_4Cl aq., extracted with diethyl ether. The organic layer was washed with brine, dried with MgSO_4 , and concentrated by rotary evaporator. The crude product was purified by column chromatography (chloroform:hexane = 1:1). White solid was obtained. The yield was 2.35 g (54%). ^1H NMR (300 MHz, CDCl_3) δ (ppm): 7.49 (s, 4H, ArH), 7.45 (s, 2H, ArH), 7.25 (d, $J = 6.0$ Hz, 2H, ArH), 7.11 (d, $J = 6.0$ Hz, 2H, ArH), 2.56 (t, $J = 6.0$ Hz, 2H, CH_2), 2.49 (s, 1H, $-\text{OH}$), 1.58 (m, 2H, CH_2), 1.27 (m, 10H, CH_2), 0.87 (t, $J = 6.0$ Hz, 3H, CH_3). ^{13}C NMR (75 MHz, CDCl_3) δ (ppm): 152.26, 142.70, 138.93, 137.57, 132.42, 128.64, 128.42, 125.23, 122.58, 121.61, 83.37, 35.74, 32.00, 31.51, 29.58, 29.54, 29.37, 22.80, 14.26. HR-MS (m/z): calcd for $\text{C}_{27}\text{H}_{28}\text{Br}_2\text{O}$, 526.0507; found, 526.0549 [M] $^+$.

2.5. Synthesis of 2,7-dibromo-9-(4-methylphenyl)-9-(4-octylphenyl)fluorene (**4**)

To a flask equipped with a stopcock were placed **3** (2.00 g, 3.92 mmol) and distilled toluene (48 mL) under nitrogen atmosphere, heated up to 60°C . After trifluoromethanesulfonic acid (0.68 mL, 7.75 mmol) was added, the mixture was stirred for 2 h. The solution was neutralized with sodium bicarbonate aq. and extracted with ethyl acetate, and the organic layer was dried with MgSO_4 . After ethyl acetate was removed by rotary evaporator, the crude product was purified by column chromatography (hexane:ethyl acetate = 30:1). White solid was obtained. The yield was 1.91 g (83%). ^1H NMR (300 MHz, CDCl_3) δ (ppm): 7.57 (d, $J = 6.0$ Hz, 2H, ArH), 7.48 (d, $J = 3.0$ Hz, 2H, ArH), 7.46 (s, 2H, ArH), 7.04 (m, $J = 3.0$ Hz, 8H, ArH), 2.55 (t, $J = 6.0$ Hz, 2H, CH_2), 2.31 (s, 3H, CH_3), 1.55 (m, 2H, CH_2), 1.27 (m, 10H, CH_2), 0.87 (t, $J = 6.0$ Hz, 3H, CH_3). ^{13}C NMR (75 MHz, CDCl_3) δ (ppm): 153.53, 141.98, 141.74, 141.69, 138.13, 136.90, 130.91, 129.51, 129.33, 128.61, 128.00, 127.95, 121.92, 121.63, 65.18, 35.65, 32.04, 31.50, 29.60, 29.38, 22.82, 21.12, 14.27. HR-MS (m/z): calcd for $\text{C}_{34}\text{H}_{34}\text{Br}_2$, 600.1027; found, 600.1088 [M] $^+$.

2.6. Synthesis of 2,7-bis(4,4,5,5-tetramethyl-1,3,2-dioxaborolan-2-yl)-9-(4-methylphenyl)-9-(4-octylphenyl)fluorene (**5**)

A solution of **4** (0.903 g, 1.5 mmol) dissolved in 10 mL of THF was added to a flask equipped with a stopcock under nitrogen atmosphere, and cooled to -78°C . Then, *n*-butyllithium (1.34 mL, 2.6 M solution in hexane) was added dropwise, and the mixture was stirred for 30 min. To this mixture, 2-isopropoxy-4,4,5,5-tetramethyl-1,3,2-dioxaborolane (1.674 g, 9.0 mmol) was added, and the mixture was stirred for 12 h. The reaction mixture was quenched with brine, and extracted with diethyl ether. The organic layer was washed with brine, dried with MgSO_4 , and concentrated by rotary evaporator. The crude product was purified by column chromatography on silica gel with hexane:ethyl acetate = 10:1 as an eluent. White solid was obtained. The yield was 0.41 g (39%). ^1H NMR (300 MHz, CDCl_3) δ (ppm): 7.81 (d, $J = 6.0$ Hz, 4H, ArH), 7.77 (d, $J = 6.0$ Hz, 2H, ArH), 7.11 (dd, $J = 3.0$ Hz, 4H, ArH), 7.01 (dd, $J = 3.0$ Hz, 4H, ArH), 2.25 (s, 3H, CH_3), 1.55 (m, 2H, CH_2), 1.31 (m, 24H, CH_3), 1.28 (m, 10H, CH_2), 0.87 (m, 3H, CH_3). ^{13}C NMR (75 MHz, CDCl_3) δ (ppm): 151.63, 143.03, 142.96, 142.90, 141.09, 135.99, 134.26, 132.47, 128.95, 128.48, 128.40, 128.23, 119.90, 119.89, 83.80, 65.01, 35.67, 32.06, 31.53, 29.62, 29.43, 25.05, 25.03, 22.81, 21.11, 14.28. Anal. Calcd for $\text{C}_{46}\text{H}_{58}\text{B}_2\text{O}_4$: C, 78.24, H, 7.08; Found: C, 78.07, H, 6.80.

2.7. Synthesis of 1-[2-(2-(2-methoxyethoxy)ethoxy)ethoxy]-4-nitrobenzene (**6**)

To a flask equipped with a Dean–Stark apparatus were placed triethylene glycol monomethyl ether (16.32 g, 0.1 mol), potassium

carbonate (33.0 g, 0.246 mol), dimethylacetamide (DMAc) (180 mL), and toluene (180 mL) and heated up to 150 °C. After water and toluene were removed completely, 4-fluoronitrobenzene (8.60 mL, 0.081 mol) was added and the mixture was stirred for 24 h. The mixture was put in ice bath and neutralized with 1 N HCl, extracted with chloroform, and the organic layer was dried with MgSO₄. After chloroform was removed by rotary evaporator, the crude product was purified by column chromatography (hexane:ethyl acetate = 1:5). Light yellow liquid was obtained. The yield was 14.04 g (93%). ¹H NMR (300 MHz, CDCl₃) δ (ppm): 8.19 (d, *J* = 6.0 Hz, 2H, ArH), 6.97 (d, *J* = 6.0 Hz, 2H, ArH), 4.21 (t, *J* = 6.0 Hz, 2H, CH₂O), 3.89 (t, *J* = 6.0 Hz, 2H, CH₂O), 3.74 (t, *J* = 6.0 Hz, 2H, CH₂O), 3.67 (m, *J* = 6.0 Hz, 2H, CH₂O), 3.65 (m, *J* = 6.0 Hz, 2H, CH₂O), 3.54 (t, *J* = 6.0 Hz, 2H, CH₂O), 3.37 (s, 2H, CH₃). ¹³C NMR (75 MHz, CDCl₃) δ (ppm): 163.71, 141.26, 125.63, 114.43, 71.66, 70.64, 70.38, 70.31, 69.14, 68.03, 58.79. HR-MS (*m/z*): calcd for C₁₃H₂₀NO₆, 286.1291; found, 286.1309 [M + H]⁺.

2.8. Synthesis of 4-{2-[2-(2-methoxyethoxy)ethoxy]ethoxy}phenylamine (**7**)

To a flask equipped with a stopcock were added **6** (5.60 g, 19.6 mmol), ethanol (108 mL), and Pd/C (0.12 g, 10% of palladium loading) under hydrogen atmosphere. After reaction for 24 h at r.t., the catalyst was removed by filtration for three times. The product was extracted by chloroform, dried with MgSO₄. After the solution was concentrated by rotary evaporator, the crude product was purified by column chromatography (hexane:ethyl acetate = 1:5). Brown liquid was obtained. The yield was 4.80 g (86%). ¹H NMR (300 MHz, CDCl₃) δ (ppm): 6.77 (d, *J* = 6.0 Hz, 2H, ArH), 6.62 (d, *J* = 6.0 Hz, 2H, ArH), 4.08 (t, *J* = 6.0 Hz, 2H, CH₂O), 3.82 (t, *J* = 6.0 Hz, 2H, CH₂O), 3.73 (t, *J* = 6.0 Hz, 2H, CH₂O), 3.67 (m, *J* = 6.0 Hz, 4H, CH₂O), 3.54 (t, *J* = 6.0 Hz, 2H, CH₂O), 3.38 (s, 2H, NH₂), 3.37 (s, 3H, CH₃). ¹³C NMR (75 MHz, CDCl₃) δ (ppm): 151.34, 140.32, 115.91, 115.48, 71.60, 70.42, 70.31, 70.22, 69.60, 67.77, 58.71.

2.9. Synthesis of (4'-bromobiphenyl-4-yl)-(4-{2-[2-(2-methoxyethoxy)ethoxy]ethoxy}phenyl)amine (**8**)

To a flask equipped with a stopcock and a condenser were placed **7** (3.00 g, 12 mmol), 4,4'-dibromobiphenyl (3.75 g, 12 mmol), sodium *tert*-butoxide (1.70 g, 1.7 mmol), Pd(dppf)Cl₂ (0.10 g, 0.12 mmol), and toluene (5 mL) under nitrogen atmosphere. After reaction for 24 h at reflux, the mixture was washed with 1 N HCl and brine. The organic layer was dried with MgSO₄, and concentrated by rotary evaporator. The crude product was purified by column chromatography (hexane:ethyl acetate = 1:5). Reddish brown solid was obtained. The yield was 2.01 g (28%). ¹H NMR (300 MHz, CDCl₃) δ (ppm): 7.53 (d, *J* = 9.0 Hz, 2H, ArH), 7.37 (d, *J* = 9.0 Hz, 4H, ArH), 7.13 (d, *J* = 9.0 Hz, 4H, ArH), 6.90 (d, *J* = 9.0 Hz, 2H, ArH), 5.71 (s, 1H, NH), 4.14 (s, 2H, CH₂O), 3.87 (t, *J* = 6.0 Hz, 2H, CH₂O), 3.76 (m, 2H, CH₂O), 3.65 (m, 4H, CH₂O), 3.57 (m, *J* = 6.0 Hz, 2H, CH₂O), 3.37 (s, 2H, CH₃). ¹³C NMR (75 MHz, CDCl₃) δ (ppm): 154.72, 145.04, 139.99, 135.50, 131.85, 130.83, 127.99, 127.84, 122.41, 120.41, 115.74, 115.64, 72.02, 70.91, 70.77, 70.67, 69.92, 67.90. HR-MS (*m/z*): calcd for C₂₅H₂₈BrNO₄, 485.1202; found, 485.1209 [M]⁺.

2.10. Synthesis of PF homopolymer (**PF1**) via nickel(0) mediated polymerization

To a 20 mL three-necked round-bottom flask equipped with a stopcock and a condenser were added **4** (0.20 g, 0.34 mmol), Ni(cod)₂ (0.20 g, 0.8 mmol), 2,2'-bipyridyl (0.12 g, 1.8 mmol), and THF (10 mL) under nitrogen atmosphere, and the mixture was stirred under reflux for 24 h. Then, **8** (0.08 g, 0.164 mmol) was

added and reflux was continued for 12 h. After the reaction chloroform was added, and the resulting solution was washed with sat. NaCl aq. and dried with MgSO₄. The solvent was removed by rotary evaporator, and the product was obtained by the precipitation into methanol and acetone. The yield was 0.13 g (89%). ¹H NMR (300 MHz, CDCl₃) δ (ppm): 7.81–7.67 (m, 2H, ArH), 7.65–7.41 (m, 4H, ArH), 7.18–6.91 (m, 8H, ArH), 4.31–3.37 (m, 16H, CH₂O), 2.58–2.42 (m, 2H, CH₂), 2.34–2.19 (m, 3H, CH₃), 1.66–1.42 (m, 2H, CH₂), 1.42–1.12 (m, 10H, CH₂), 0.85–0.91 (m, 3H, CH₃).

2.11. Synthesis of PF homopolymer (**PF2**) via Suzuki coupling polymerization

To a 20 mL three-necked round-bottom flask equipped with a stopcock and a condenser were added **4** (0.166 g, 0.276 mmol), **5** (0.226 g, 0.324 mmol), Pd(PPh₃)₄ (3.46 mg, 0.003 mmol, 0.5%), 2N K₂CO₃ aq. (4 mL), and toluene (4 mL) under nitrogen atmosphere, and the mixture was refluxed for 48 h. Then, **8** (0.15 g, 0.3 mmol) was added and reflux was continued for 12 h. After the reaction, chloroform was added, the resulting solution was washed with sat. NaCl aq. and dried with MgSO₄. The solvent was removed by rotary evaporator, the product was obtained by precipitation into methanol. The yield was 0.221 g (83%). ¹H NMR (300 MHz, CDCl₃) δ (ppm): 7.81–7.67 (m, 2H, ArH), 7.65–7.41 (m, 4H, ArH), 7.18–6.91 (m, 8H, ArH), 4.31–3.37 (m, 16H, CH₂O), 2.58–2.42 (m, 2H, CH₂), 2.34–2.19 (m, 3H, CH₃), 1.66–1.42 (m, 2H, CH₂), 1.42–1.12 (m, 10H, CH₂), 0.85–0.91 (m, 3H, CH₃). The homopolymers **PF4** and **PF5** were synthesized by the same procedure as **PF2** with different feed ratios of **4** and **5**. The yield of **PF4** was 0.210 g (79%); that of **PF5** was 0.226 g (85%).

2.12. Synthesis of PF homopolymer (**PF3**) via one-pot Suzuki coupling polymerization

To a 20 mL three-necked round-bottom flask equipped with a stopcock and a condenser were added **4** (0.337 g, 0.56 mmol), bis(pinacolato)diboron (0.166 g, 0.655 mmol), Pd(PPh₃)₄ (3.2 mg, 0.0028 mmol, 0.5 mol%), 2N K₂CO₃ aq. (3 mL), and toluene (3 mL) under nitrogen atmosphere and the mixture was refluxed for 48 h. Then, **8** (0.15 g, 0.3 mmol) was added and reflux was continued for 12 h. After the reaction chloroform was added, the resulting solution was washed with sat. NaCl aq. and dried with MgSO₄. The solvent was removed by rotary evaporator, and the product was obtained by precipitation into methanol. The yield was 0.176 g (71%). ¹H NMR (300 MHz, CDCl₃) δ (ppm): 7.81–7.67 (m, 2H, ArH), 7.65–7.41 (m, 4H, ArH), 7.18–6.91 (m, 8H, ArH), 4.31–3.37 (m, 16H, CH₂O), 2.58–2.42 (m, 2H, CH₂), 2.34–2.19 (m, 3H, CH₃), 1.66–1.42 (m, 2H, CH₂), 1.42–1.12 (m, 10H, CH₂), 0.85–0.91 (m, 3H, CH₃).

2.13. Synthesis of PF-*b*-PTPA block copolymer (**PF-PTPA2**)

To a 10 mL two-necked round-bottom flask equipped with a stopcock and a condenser were added **PF2** (0.134 g, 0.30 mmol of repeating unit), **8** (0.146 g, 0.3 mmol), P(*t*-Bu)₃ (7.5 μL, 0.01 mmol), Pd(OAc)₂ (0.0014 g, 0.006 mmol), *t*-BuONa (0.032 g, 0.33 mmol), and THF (3 mL) under nitrogen atmosphere and the mixture was stirred under reflux for 24 h. After the reaction, the resulting solution was washed by chloroform. After removing the solvent by rotary evaporator, the product was obtained by precipitation into methanol and acetone. The yield of **PF-PTPA2** was 0.199 g (48%). **PF-PTPA4** and **PF-PTPA5** were synthesized by the same procedure with different feed ratios. **PF-PTPA4** was synthesized from **PF4** (0.094 g, 0.21 mmol of repeating unit), **8** (0.0243 g, 0.05 mmol), P(*t*-Bu)₃ (1.5 μL, 0.005 mmol), Pd(OAc)₂ (0.0003 g, 0.001 mmol), *t*-BuONa (0.006 g, 0.055 mmol), and THF (2 mL). The yield was

0.147 g (53%). **PF-PTPA5** was synthesized from **PF5** (0.132 g, 0.30 mmol of repeating unit), **8** (0.146 g, 0.3 mmol), P(*t*-Bu)₃ (7.5 μ L, 0.01 mmol), Pd(OAc)₂ (0.0014 g, 0.006 mmol), *t*-BuONa (0.032 g, 0.33 mmol), and THF (3 mL). The yield was 0.194 g (47%).

2.14. Characterizations

¹H and ¹³C NMR spectra were obtained on a JEOL ALPHA300 instrument at 300 MHz at 25 °C. Deuterated chloroform was used as a solvent with tetramethylsilane as an internal standard. Number- and weight-average molecular weights (*M*_n and *M*_w) and polydispersity index (PDI) were determined by gel permeation chromatography (GPC) analysis with a JASCO RI-2031 detector eluted with chloroform at a flow rate of 0.5 ml/min at room temperature and calibrated by standard polystyrene samples. Thermogravimetric analysis (TGA) and Differential scanning calorimetry (DSC) analysis was performed on a Rigaku DSC-8230 under nitrogen atmosphere at heating and cooling rates of 10 °C/min. UV–vis absorption spectra were obtained on a JASCO V-570 spectrophotometer and fluorescence spectra were obtained with JASCO FP-6500 spectrophotometer with an excitation at 380 nm. Cyclic voltammetry (CV) was conducted on a Niko Keisoku Model NPGFZ-2501-A potentiogalvanostat. All measurements were carried out at room temperature in a typical three-electrode cell with a working electrode (glassy carbon electrode), a reference electrode (Ag/AgCl), and a counter electrode (Pt wire) at a scanning rate of 0.1 V/s. In all measurements, acetonitrile and tetrabutylammonium tetrafluoroborate (Bu₄NBF₄) (0.1 M) were used as solvent and supporting electrolyte, respectively.

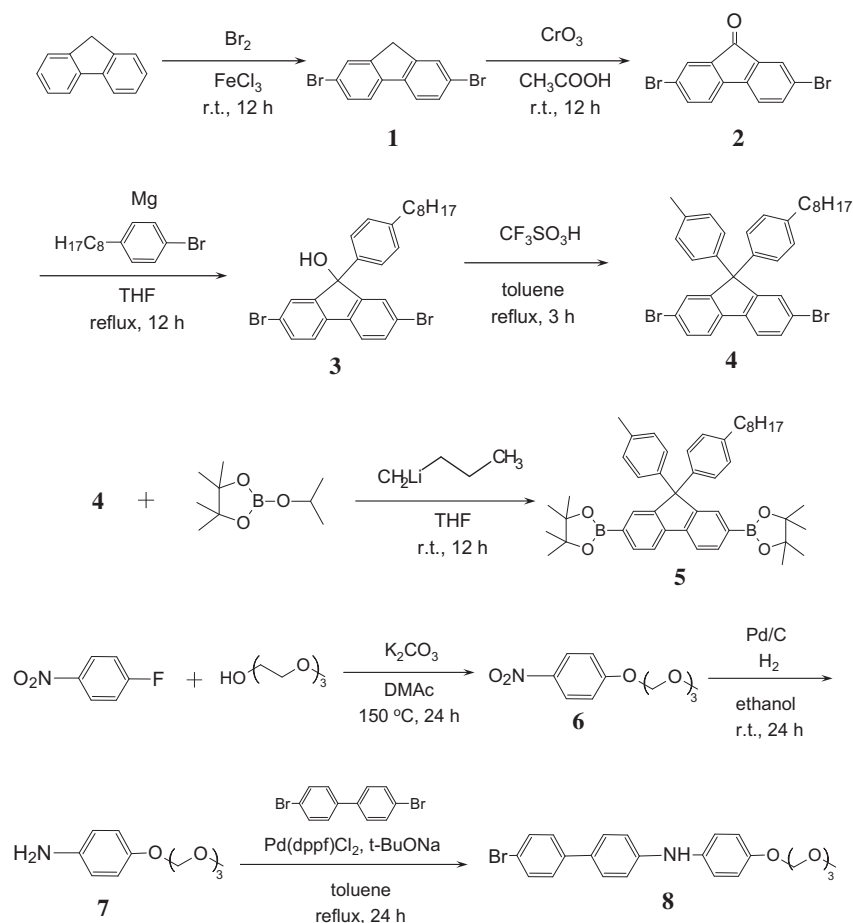
2.15. Device fabrication

Prior to preparation of device, a glass slide with indium tin oxide (ITO) patterns was washed by an alkaline cleaner under sonication and rinsed with deionized water. The substrate was subsequently washed by 2-propanol under sonication, rinsed with clean 2-propanol, and dried with nitrogen. PEDOT:PSS with 30 nm of thickness was spin-coated on the substrate at 2500 rpm from the dispersion in water filtered by 0.2 μ m of membrane filter, followed by annealing at 200 °C for 1 h. Polymer layer was laminated on PEDOT:PSS by spin-coating at 500 rpm for 30 s from chlorobenzene solution (12 mg/mL) filtered by 0.45 μ m of membrane filter, and annealed at 120 °C for 1 h under nitrogen atmosphere. On the polymer, 2,9-dimethyl-4,7-diphenyl-1,10-phenanthroline (BCP) with 50 nm thickness was deposited by thermally evaporation in carbon pot at 240 °C under vacuum with a rate of 1.5 Å/s. As a cathode, lithium fluoride with 0.5 nm of thickness followed by a Al with 100 nm of thickness was deposited on the organic layer with a rate of 0.1 Å/s and a rate of 4.5 Å/s using tantalum and tungsten boats, respectively. Finally, the polymer device was set into a metal can with barium oxide as a drying agent under a nitrogen atmosphere, and passivated with an epoxy resin (XNR 5570-B1, Nagase ChemteX Corporation) irradiated by UV light.

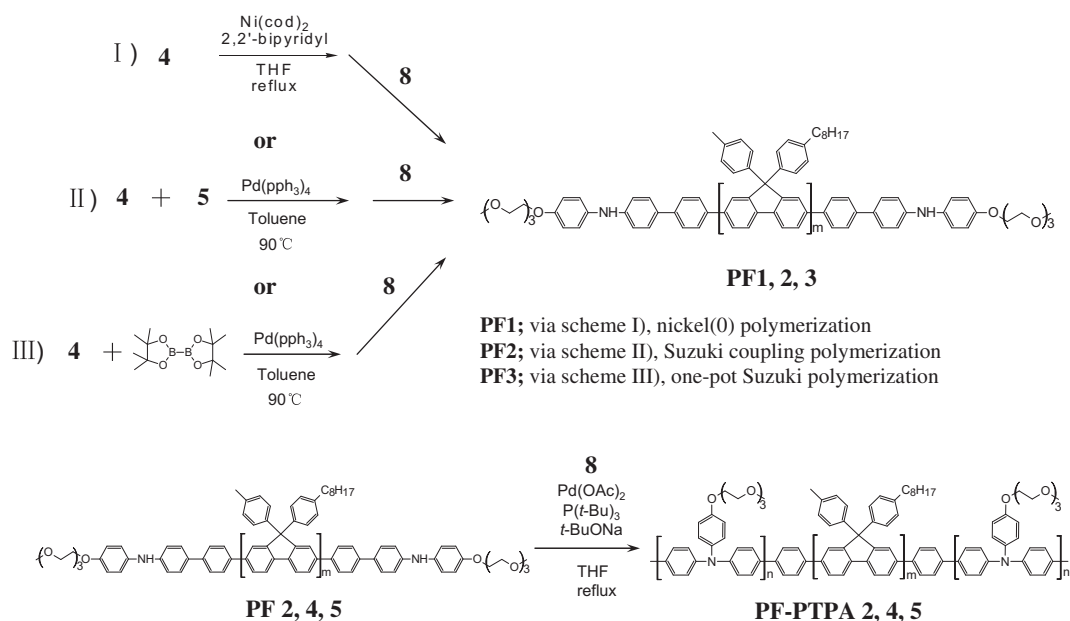
3. Result and discussion

3.1. Synthesis and characterization

Scheme 1 illustrated the synthetic route of 2,7-dibromo-9-(4-methylphenyl)-9-(4-octylphenyl)fluorene (**4**) and (4'-



Scheme 1. Synthetic route for monomers.



Scheme 2. Synthetic route for PF homopolymers and PF-PTPA block copolymers.

bromobiphenyl-4-yl)-(4-{2-[2-(2-methoxyethoxy)ethoxy]ethoxy}phenyl)amine (**8**), monomers for polyfluorene and poly(triphenylamine) backbones, respectively. In order to avoid the formation of aggregates/excimers and suppress interchain interactions in PF, octylphenyl and methylphenyl groups were introduced at the 9-position of fluorene in **4**. In the meantime, TPA monomer **8** was modified with tri(ethylene oxide) (TEO) group, which is considered to predominantly interact with hydrophilic PEDOT/PSS layer in EL device to prevent the migration of an impurity from PEDOT/PSS layer to PF emitting layer by the formation of poly(triphenylamine) skin layer between them. Since Suzuki coupling reaction was utilized for the preparation of PF, 2,7-bis(4,4,5,5-tetramethyl-1,3,2-dioxaborolan-2-yl)-9-(4-methylphenyl)-9-(4-octylphenyl)fluorene (**5**) were synthesized from **4** using *n*-butyllithium and 2-isopropoxy-4,4,5,5-tetramethyl-1,3,2-dioxaborolane.

In order to prepare the PF homopolymer with diphenylamine group at terminals, nickel(0) mediated polymerization of **4** (**PF1**) and Suzuki coupling polymerization of **4** and **5** (**PF2**) were conducted as shown in Scheme 2. One-pot Suzuki coupling polymerization of **4** in the presence of bis(pinacolato)diboron was also carried out (**PF3**). At the end of polymerizations, the terminals of the PFs were converted to the diphenylamine moiety by the coupling reaction with **8**.

The resulting molecular weights of PF homopolymers were summarized in Table 1. The polymers **PF1**, **PF2**, and **PF3** exhibited similar M_n ranging from 9700 to 13400. However, the PDI (M_w/M_n) value of **PF1** was 5.80, higher than those of the other two homopolymers (2.42 and 2.19). Therefore, it was difficult to control the

molecular weight and to convert the terminal into the diphenylamine group completely. Furthermore, the tedious removal of the large amount of nickel residue is required. In contrary, for **PF2** prepared by Suzuki coupling polymerization, the molecular weight of the polymer could be easily controlled by changing the molar ratio of reactant monomers. Moreover, the palladium complex as well as other residues could be removed simply by washing the products with water and methanol. The terminals of **PF2** were designed to be boronic ester by utilizing excess amount of monomer **5**, and successfully converted to diphenylamine group at the end of polymerization. Because of troublesome preparation of boronic-acid-ester monomers, more facile one-pot Suzuki coupling polymerization was reported recently [28]. Therefore, **PF3** was synthesized via one-pot Suzuki coupling polymerization by means of simply replacing **5** with bis(pinacolato)diboron without changing any reaction conditions. The polymer was obtained in moderate yield, and the molecular weight and polydispersity of **PF3** were similar to conventionally prepared **PF2**. However, the terminal modification into diphenylamine group by coupling with **8** was failed.

For the synthesis of PF with the terminals modification into diphenylamine group, Suzuki coupling polymerization is a prior selection to nickel(0) mediated polymerization. Therefore, we prepared PFs with various molecular weights, and these homopolymers were used for the synthesis of block copolymers. It is well known that the molecular weight of polymers in polycondensation can be varied by deviating from the stoichiometry between two monomers [29]. Changing molar ratio of bromo-group/boronic-

Table 1
Characterizations of PF homopolymers prepared by various polymerization methods.

Polymer	Molar ratio [4]/[5]	M_n^a	PDI ^a	Yield (%)	T_g (°C)	T_d (°C)	λ_{max} (UV-vis)		λ_{max} (PL)	
							Solution (nm)	Film (nm)	Solution (nm)	Film (nm)
PF1	1/0	9700	5.80	89	104	464	387	385	416	423
PF2	0.92/1.08	13400	2.42	83	111	450	388	383	417	418
PF3	0.92/1.08 ^b	10800	2.19	71	107	445	387	384	417	421

^a Determined by GPC.

^b Molar ratio of [4]/[bis(pinacolato)diboron].

Table 2
Characterizations of PF-PTPA block copolymers.

polymer	Molar ratio 4/5	Molar ratio ^a in feed in polymer	M_n^b	PDI ^b	Yield (%)	T_d (°C)
PF2	0.92/1.08	–	13400	2.42	83	450
PF-PTPA2	–	50/50 55/45	23100	2.67	48	415
PF4	0.95/1.05	–	18700	3.24	79	448
PF-PTPA4	–	81/19 89/11	20500	2.72	53	410
PF5	0.98/1.02	–	26400	3.48	85	451
PF-PTPA5	–	50/50 65/35	43400	3.28	47	401
PTPA	–	–	9700	2.80	94	406

^a Molar ratio of PF repeating unit to 8.

^b Determined by GPC.

ester-group to 0.95/1.05 and 0.98/1.02, polyfluorene homopolymers **PF4** and **PF5** were prepared via Suzuki coupling reaction. The C–N coupling polymerization of **8** in the presence of these three PFs was conducted to obtain polytriphenylamine-*block*-polyfluorene-*block*-polytriphenylamine triblock copolymers, **PF-PTPA2**, **PF-PTPA4**, and **PF-PTPA5** (Scheme 2). The feed ratios of the monomers and the resulting molecular weights of the polymers were summarized in Table 2. The M_n increased after the polymerization of **8** compared with those of PF homopolymers. The polymer structure was confirmed by ¹H NMR spectra. For example, in Fig. 1, the signals assignable to methylene protons derived from TEO chain were observed at 3.3–4.1 ppm, clearly indicating that TPA monomer **8** was introduced at the ends of PF backbone. The molar ratio of the repeating unit of block copolymers were calculated from ¹H NMR spectra, depending on the area integral of ether proton and aliphatic proton (shown in Fig. SI-5). The molar ratio of fluorene/TPA units in **PF-PTPA2**, **PF-PTPA4** and **PF-PTPA5** were determined as 55/45, 89/11, 65/35, respectively. The GPC chromatograms of block copolymers showed unimodal profiles and a shift to higher molecular weight from homopolymers (Fig. SI-1). This indicates that no PTPA homopolymer remained in the block copolymers. PDI values of the six polymers were in the range from 2.42 to 3.48. All the polymers are soluble in common organic solvents such as chloroform and THF, and formed the thin films by solution processing.

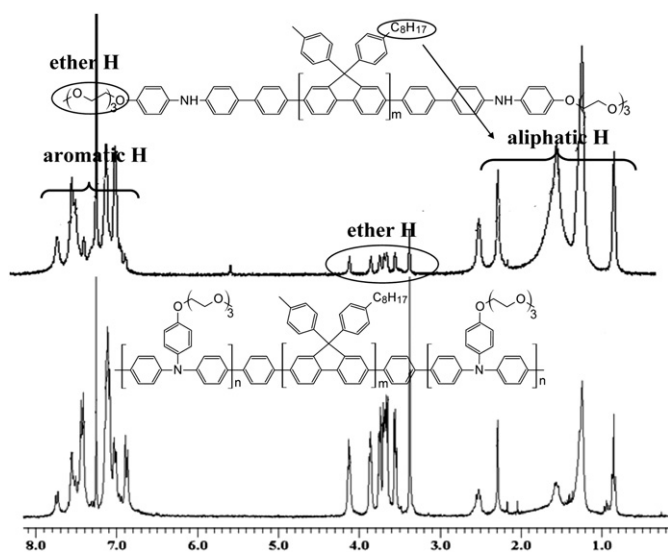


Fig. 1. ¹H NMR spectra of PF2 and PF-PTPA2.

3.2. Thermal properties

The glass transition temperature (T_g) of the polymers was measured by DSC under N_2 atmosphere at a scan rate of 10 °C/min. The homopolymers, **PF2**, **PF4**, and **PF5** showed a T_g of 111, 118, and 127 °C, respectively. The T_g value slightly increased with an increase of the molecular weight. Fig. 2 shows DSC thermograms of **PF5**, **PTPA**, and **PF-PTPA5**. **PTPA** homopolymer exhibited relatively high T_g of 175 °C. **PF-PTPA5** showed two distinct transitions at 119, and 173 °C, corresponding to T_g s of PF and PTPA, respectively, which indicates the microphase-separated structure. Other block copolymers, (**PF-PTPA2**, **PF-PTPA4**) also showed double T_g s.

3.3. Optical properties

The optical properties of PF homopolymers and PF-PTPA block copolymers in chloroform solution and in film state were shown in Fig. 3 and Table 3. In the absorption spectra of solution state, both homopolymers and block copolymers showed $\lambda_{abs,max}$ of 387–389 nm. Similar results were obtained in film state. All the polymers exhibited similar PL spectra in solution state, having distinct vibronic bands at about 418 and 445 nm and a shoulder around 470 nm upon excitation at 380 nm. This is attributed to the fact that the distance between polymer main chains in dilute solution is sufficient to make interchain interactions negligible. In the film state, similar emission behavior was observed in all of the polymers (not only PF homopolymers but also PF-PTPA block copolymers) indicating that the attachment of PTPA block to the PF backbone gives little influence on the luminescent properties of PF, although the emission peak width for block copolymers was slightly increased. As Jin et al. reported, random copolymers consisting of PF and tetraphenylbenzidine moieties show a red-shifted emission compared with PF [5]. Taking the fact into consideration that extensive broadening was observed in lowest molecular weight of **PF-PTPA2**, peak broadening is probably resulted from the existence of junction unit between PF and PTPA.

3.4. Electrochemical properties

The electrochemical properties of the polymers were investigated by cyclic voltammetry (CV). As shown in Fig. SI-3a, the oxidation process of PF homopolymers started at around 1.40 V, and the reversible redox peaks in the reduction process appear at around –0.80 V. The oxidation onset and the reduction potential for homopolymers **PF2**, **PF4**, and **PF5** slightly changed because they possess the same PF main chain structure with an increase of molecular weight. The same result was also found in the case of PF-

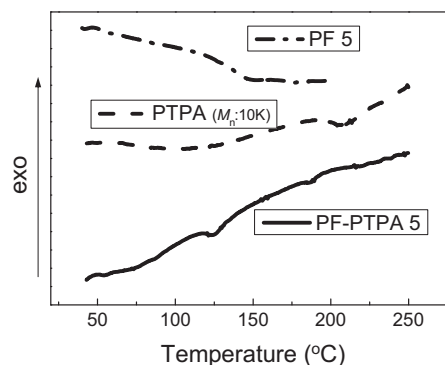


Fig. 2. DSC profiles of PF, PTPA and PF-PTPA.

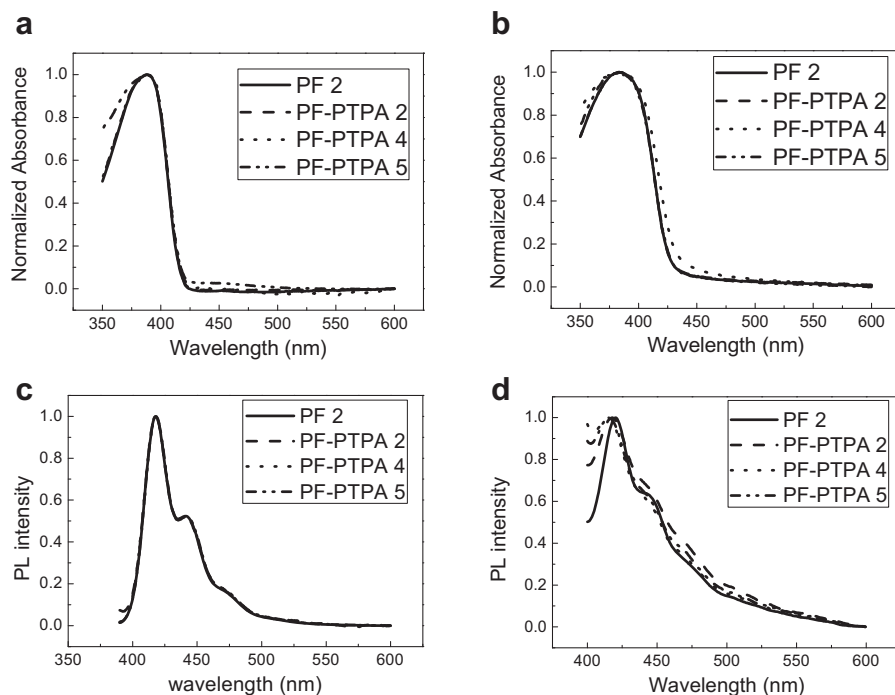


Fig. 3. Optical properties of PF2 and PF-PTPAs: (a) UV, soln.; (b) UV, film; (c) PL, soln.; (d) PL, film.

PTPA block copolymers (Fig. SI-3b) except that a new oxidation peaks in the anodic sweep were observed at around 0.90 V. CV data for block copolymers were basically coincident with those of the previously reported polymers with fluorene and triphenylamine backbone [30,31]. All of PF-PTPA block copolymers exhibited a decreased oxidation onset in comparison with corresponding PF homopolymers, which attributed to attached PTPA segment. Furthermore, the oxidation potential of all of block copolymers slightly increased as the PTPA segment length increased.

The energy levels of the highest occupied molecular orbital (HOMO) of the polymers were estimated from their oxidation potential according to an empirical formula, $E_{\text{HOMO}} = -e(E_{\text{ox}} + 4.4)$ V. HOMO levels of PF homopolymers were in the range of from -5.79 to -5.88 eV, deeper than those of PF-PTPA block copolymers, from -5.29 to -5.33 eV. The results indicated that the introduction of polytriphenylamine segment into the polymer chain ends efficiently raised their HOMO levels, thus could facilitate the hole injection and transport from an anode to the emitting polymer. The levels of the lowest unoccupied molecular orbital (LUMO) for the polymers were calculated with the reduction potential E_{red} from the empirical formula $E_{\text{LUMO}} = -e(E_{\text{red}} + 4.4)$ V.

The electrical band gaps (E_{g}^{el}) of the polymers were estimated by subtracting the HOMO levels from their respective LUMO energies. The electrochemical properties in films were summarized in Table 3.

Fig. 4 showed the energy level diagram for PF2 and PF-PTPA2 compared with ITO as an anode and widely used PEDOT/PSS as a hole-injection-layer material. The HOMO levels of PF-PTPA block copolymers suitably match the work function of PEDOT/PSS (-5.2 eV), while there was an energy barrier over 0.50 eV between the HOMO of PEDOT/PSS and those of PF homopolymers. This suggests that a facile hole injection from ITO/PEDOT/PSS into PF-PTPA layer can be expected in comparison with PF.

3.5. EL properties

The performance of the EL devices based on PF homopolymers and PF-PTPA block copolymers with the device structure of ITO/PEDOT:PSS/polymer/BCP/LiF/Al was evaluated. Fig. 5 showed current density vs. voltage, luminance vs. current density, and current efficiency vs. current density characteristics. As shown in Fig. 5a, the current density of devices based on PF-PTPA block

Table 3
Optical and electrochemical properties of PFs and PF-PTPAs.

Polymer	λ_{max} (UV-vis)		λ_{max} (PL)		E_{ox} (V)	E_{red} (V)	E_{HOMO} (-eV) ^a	E_{LUMO} (-eV) ^b	E_{g}^{el} (eV) ^c
	Solution (nm)	Film (nm)	Solution (nm)	Film (nm)					
PF2	388	383	417	418	1.39	-0.79	5.79	3.61	2.18
PF-PTPA2	389	386	418	416	0.89	-0.74	5.29	3.66	1.63
PF4	388	386	418	421	1.40	-0.82	5.80	3.58	2.22
PF-PTPA4	389	384	418	415	0.85	-0.71	5.25	3.69	1.56
PF5	389	385	419	420	1.48	-0.85	5.88	3.55	2.33
PF-PTPA5	386	383	418	416	0.93	-0.79	5.33	3.61	1.72

^a $E_{\text{HOMO}} = -e(E_{\text{ox}} + 4.4)$ V.

^b $E_{\text{LUMO}} = -e(E_{\text{red}} + 4.4)$ V.

^c Electrical band gap: $E_{\text{g}}^{\text{el}} = \text{LUMO} - \text{HOMO}$.

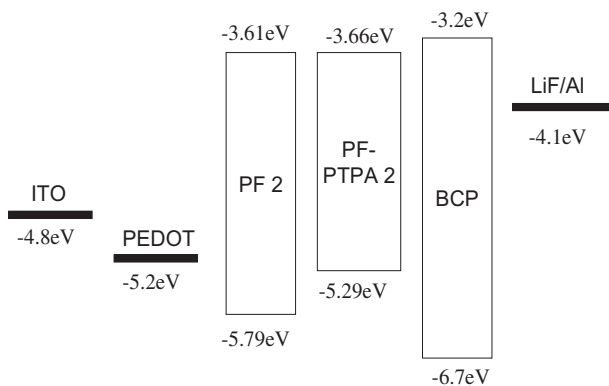


Fig. 4. Energy level diagram of PF2 and PF-PTPA2.

copolymers was higher than that from corresponding PF homopolymers. Moreover, with the PTPA content increased, the current density of devices of block copolymers increased (**PF-PTPA2** > **PF-PTPA5** > **PF-PTPA4** > **PFs**). This fact indicates that with the increase of PTPA content, the hole injection and transport in PF-PTPA layer was improved more efficiently. The luminance of all the polymers was exponentially increased with an increase in voltage. At the similar current density (for example, 30 mA/cm²), **PF-PTPA2**, **PF-PTPA4**, and **PF-PTPA5** showed higher luminance (532, 433, and 586 cd/m²) than corresponding PF homopolymers (285, 226, and 274 cd/m²), respectively. Moreover, similar results were obtained for the maximum luminance. The maximum current efficiencies of PF homopolymers were from 1.14 to 1.21 cd/A, whereas those of PF-PTPA block copolymers increased from 1.60 to 2.27 cd/A. The improvement of the device performance using block copolymers is probably attributed to an efficient hole injection, which leads good balance between hole and electron charges in the emitting layer, by the attachment of PTPA block to PF backbone. In

addition, it is suggested that the microphase-separated structure created by the block copolymers offered large interface between PF and PTPA segments for the efficient charge recombination [25]. The difference of polarity between PF and PTPA with TEO moiety may promote the microphase separation, which also contributes the improvement of current efficiency.

Although PF homopolymers possesses the different molecular weights, they showed similar device performances (both luminance and current efficiency). It also should be noted that, although **PF-PTPA2**, **PF-PTPA4** and **PF-PTPA5** possesses different PTPA repeating units ($n = 15, 5, \text{ and } 30$), there was nearly no difference in the UV–vis and PL spectrum and a slight variation in the electrochemical properties. However, the EL device based on **PF-PTPA2** and **PF-PTPA5** exceeded that of **PF-PTPA4** in the electroluminescent properties. For the three block copolymers **PF-PTPA2**, **PF-PTPA4**, and **PF-PTPA5**, the ratios of PF/PTPA units are roughly calculated as 55/45, 89/11, and 65/35, respectively. With the PTPA content increased, both luminance and current efficiency increased (**PF-PTPA2** > **PF-PTPA5** > **PF-PTPA4**).

The EL spectra of the devices based on **PF2** and PF-PTPA block copolymers were shown in Fig. 6, and their corresponding CIE coordinates were summarized in Table 4. All the devices based on block copolymers exhibited a blue emission without unnecessary green-emitting bands. As shown in Table 4, PF homopolymers exhibit EL emission with CIE coordinates ranging from (0.17, 0.20) to (0.18, 0.21); while PF-PTPA block copolymers showed slightly deeper blue color with CIE coordinates ranging from (0.16, 0.18) to (0.17, 0.19). The EL profiles of PF-PTPA block copolymers were slightly narrow compared with that of **PF2** as the result of suppression of the undesired emission at 460–550 nm by the incorporation of PTPA segment [32]. The influence of PTPA content on the EL spectra and color purities of devices based on block copolymers was not observed obviously. We noted that the dominating contribution of EL properties comes from emission peak at 450 nm, which was slightly red-shifted from that of PL emission (425 nm) [32].

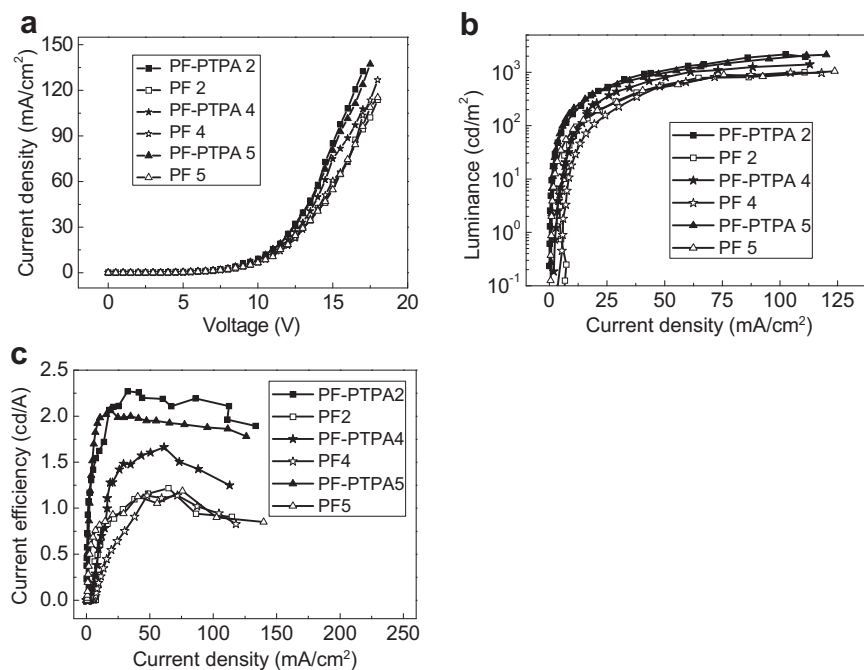


Fig. 5. Device characteristics of blue-emitting PLEDs, (a) current density – voltage characteristics; (b) luminance – current density characteristics; (c) current efficiency – current density characteristics.

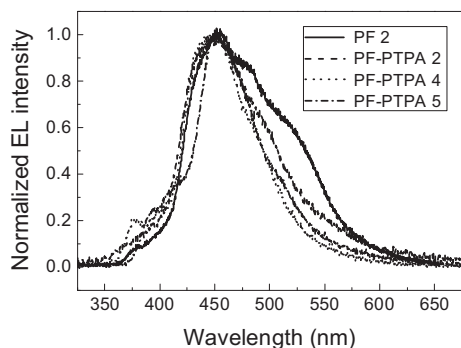


Fig. 6. Electroluminescence spectra of devices based on PF2 and PF-PTPAs at 14V.

Table 4
Device performance of PFs and PF-PTPAs.

Polymer	Luminance at 30 mA/cm ² (cd/m ²)	Maximum luminance (cd/m ²)	Maximum current efficiency (cd/A)	Color coordinate [x, y]
PF2	285	1001	1.21	0.17, 0.20
PF-PTPA2	532	2160	2.27	0.16, 0.18
PF4	226	984	1.14	0.17, 0.21
PF-PTPA4	433	1409	1.60	0.16, 0.19
PF5	274	1050	1.19	0.18, 0.21
PF-PTPA5	586	2136	2.07	0.17, 0.19

4. Conclusions

In order to prepare polyfluorene block copolymers containing hole transporting segments for PLED devices, 2,7-dibromo-9-(4-methylphenyl)-9-(4-octylphenyl)fluorene and (4'-bromobiphenyl-4-yl)-(4-{2-[2-(2-methoxyethoxy)ethoxy]ethoxy}phenyl)amine were synthesized as novel monomers for PF and PTPA backbone. For the preparation of polyfluorene homopolymer, Suzuki coupling polymerization was selected, and the terminals were precisely converted to diphenylamine group. PTPA block was introduced at the terminals of PF via C-N coupling polymerization to give PTPA-block-PF-block-PTPA triblock copolymers (PF-PTPAs) with different PTPA chain lengths. These polymers showed good solubility in common organic solvents, had good thermal stability, and readily formed thin film by solution processing. All of the polymers exhibited an absorption peak at around 385 nm both in chloroform solution and in film state, while the PL emission were observed at around 420 nm, the range of blue-light wavelength. The photo-physical analysis revealed that the PTPA chains gave no influence on the blue emission of PF segment. PF-PTPA block copolymers showed relatively high HOMO level at around -5.3 eV compared with those of PF by CV measurement, which provided a good match with the work function of PEDOT/PSS (-5.2 eV). This suggests a facile hole injection from ITO/PEDOT/PSS into the HOMO of PF-PTPA than PF. The EL devices based on PF-PTPA block copolymers

showed higher luminance and current efficiency than those of corresponding PF homopolymers. While PF homopolymers showed similar device performances with different molecular weights, device performance of PF-PTPA block copolymers increased with the PTPA content increased. These results indicates that the incorporation of hole transporting PTPA segments into PF backbone improved the hole injection into PF emitting layer, which offered the effective charge recombination.

Appendix. Supporting information

Supporting information related to this article can be found online at doi:10.1016/j.polymer.2012.02.021.

References

- [1] Lim E, Jung BJ, Shim HK. *J Polym Sci Part A Polym Chem* 2006;44:243–53.
- [2] Cho NS, Park JH, Lee SK. *Macromolecules* 2006;39:177–83.
- [3] List EJV, Gunter R, Scandiucci de Freitas P, Scherf U. *Adv Mater* 2002;14:374–8.
- [4] Romaner L, Pogantsch A, Freitas PS, Scherf U, Gaal M, Zojer E, et al. *Adv Funct Mater* 2003;13:597–601.
- [5] Jin JK, Kwon SK, Kim YH. *Macromolecules* 2009;42:6339–47.
- [6] Bolognesi A, Betti P, Botta C, Destri S. *Macromolecules* 2009;42:1107–13.
- [7] Kreyenschmidt M, Klarner G, Fuhrer T, Ashenurst J, Karg S, Chen WD, et al. *Macromolecules* 1998;31:1099–103.
- [8] Lee JI, Klarner G, Miller RD. *Chem Mater* 1999;11:1083–8.
- [9] Gong X, Iyer PK, Moses D, Bazan GC, Heeger AJ, Xiao SS. *Adv Funct Mater* 2003;13:325–30.
- [10] Klarner G, Lee JI, Lee VY, Chan E, Chen JP, Nelson A, et al. *Chem Mater* 1999;11:1800–5.
- [11] Zhang QS. *Chin J Chem* 2010;28:1482–6.
- [12] Lee SK, Ahn T, Cho NS. *J Polym Sci Part A Polym Chem* 2007;45:1199–209.
- [13] Tang CW, VanSlyke SA. *Appl Phys Lett* 1987;51:913–5.
- [14] Adachi C, Tsutsui T, Saito S. *Appl Phys Lett* 1989;55:1489–91.
- [15] Kuwabara Y, Ogawa H, Inaba H, Noma N, Shirota Y. *Adv Mater* 1994;6:677–9.
- [16] Noda T, Ogawa H, Noma N, Shirota Y. *Adv Mater* 1997;9:720–2.
- [17] Ogino K, Kanegae A, Yamaguchi R, Sato H, Kurjata J. *Macromol Rapid Commun* 1999;20:103–6.
- [18] Nomura M, Shibasaki Y, Ueda M, Tugita K, Ichikawa M, Taniguchi Y. *Macromolecules* 2004;37:1204–10.
- [19] Ishikawa M, Kawai M, Ohsawa Y. *Synth Met* 1991;40:231–8.
- [20] Tanaka S, Iso T, Doke Y. *Chem Commun*; 1997:2063–4.
- [21] Tsuchiya K, Shimomura T, Ogino K. *Polymer* 2009;50:95–101.
- [22] Duan L, Chin BD, Yang NC, Kim MH, Lee ST, Chung HK. *Synth Met* 2007;157:343–6.
- [23] Tsuchiya K, Kasuga H, Kawakami A, Taka H, Kita H, Ogino K. *J Polym Sci Part A Polym Chem* 2010;48:1461–8.
- [24] Tsuchiya K, Sakaguchi K, Kasuga H, Kawakami A, Taka H, Kita H, et al. *Polymer* 2010;51:616–22.
- [25] Tsuchiya K, Sakaguchi K, Kawakami A, Taka H, Kita H, Ogino K. *Synth Met* 2010;160:1679–82.
- [26] Ma B, Kim BJ, Deng L, Poulsen DA, Thompson ME, Fréchet JMJ. *Macromolecules* 2007;40:8156–61.
- [27] Lu S, Liu TX, Ke L, Ma DG, Chua SJ, Huang W. *Macromolecules* 2005;38:8494–502.
- [28] Walczak RM, Brookins RN, Savage AM, VanderAa EM, Reynolds JR. *Macromolecules* 2009;42:1445–7.
- [29] Schlüter AD, Wegner G. *Acta Polym* 1993;44:59–69.
- [30] Redecker M, Bradley DDC, Inbasekaran M, Wu WW, Woo EP. *Adv Mater* 1999;11:241–6.
- [31] Sancho-Garcia JC, Foden CL, Grizzi I, Greczynski G, de Jong MP, Salaneck WR, et al. *J Phys Chem B* 2004;108:5594–9.
- [32] Lu LP, Kabra D, Jhonson K, Friend RH. *Adv Funct Mater* 2012;22:144–50.